REGULAR ARTICLE

Combining molecular dynamics with Monte Carlo simulations: implementations and applications

Erik C. Neyts · Annemie Bogaerts

Abstract In this contribution, we present an overview of the various techniques for combining atomistic molecular dynamics with Monte Carlo simulations, mainly in the context of condensed matter systems, as well as a brief summary of the main accelerated dynamics techniques. Special attention is given to the force bias Monte Carlo technique and its combination with molecular dynamics, in view of promising recent developments, including a definable timescale. Various examples of the application of combined molecular dynamics / Monte Carlo simulations are given, in order to demonstrate the enhanced simulation efficiency with respect to either pure molecular dynamics or Monte Carlo.

Keywords Molecular dynamics · Monte Carlo · Long time scale dynamics

1 Introduction

In order to gain control over properties of and processes in materials, an atomic scale understanding is of primary importance. To this end, two main techniques are commonly used, viz. molecular dynamics (MD) and Monte Carlo (MC) simulations [1].

Molecular dynamics (MD) simulations have been shown to be an invaluable tool to investigate both static and dynamic properties of systems at the atomic scale. Consequently, they have been applied to a countless number of systems and processes, ranging from the calculation of structural and morphological properties of materials [2, 3], transport properties [4], growth of thin films and other nanomaterials [5, 6], protein folding [7], etching [8, 9], sputtering [10], chemical reactions [11], friction [12], fraction [13], phase changes [14, 15] and so forth.

Classical MD simulations are based on solving the equations of motion for all particles in the system to obtain the trajectory of the particles in phase space. Thus, essentially, the integration of these equations yields the positions and velocities of the particles, as well as the forces acting on them. The forces are derived from some suitable interatomic potential. This has two immediate implications. First, classical MD simulations are approximative, due to the inexact nature of the calculated forces and energies. Second, exactly because of this approximative nature, they are computationally cheap, making calculations of systems containing millions of atoms feasible, in contrast to more exact approaches such as Car-Parrinello MD. Also, the timescale that can be handled is orders of magnitude longer than what is possible with more exact approaches.

On the other hand, MD simulations are limited in two main respects. First, while the system may contain up to millions of atoms, this still only constitutes a material on the nanometer to sub-micrometer scale at typical solid-state and liquid densities. This makes it difficult to study, for instance, grain boundaries in a polycrystallite [16]. A second, more severe restriction, is the timescale that can be reached. Here, the typical limit is in the nanosecond–microsecond timescale, although in exceptional cases the (sub-)millisecond range may be reached [17]. This makes it difficult to simulate, for instance, the growth of a material, which typically occurs on timescales well beyond this limit.

E. C. Neyts (✉) · A. Bogaerts
Department of Chemistry, University of Antwerp,
PLASMANT Research Group, Universiteitsplein 1,
Antwerp 2610, Belgium
e-mail: erik.neyts@ua.ac.be

A number of so-called accelerated molecular dynamics techniques have been developed to extend the timescale of MD simulations, as will be discussed in Sect. 2.

An alternative to MD for studying atomic scale processes and calculating material properties is the use of Monte Carlo methods [1]. In a Monte Carlo (MC) simulation, atoms are displaced based on random numbers. Thus, in contrast to MD, the MC technique is not deterministic. The most famous MC technique is undoubtedly Metropolis MC (MMC) [18]. The MMC algorithm leads to a system in equilibrium, corresponding to the Boltzmann distribution. Note, however, that the path toward this equilibrium is not necessarily physical (and usually it is indeed not). Indeed, whereas a MD simulation typically generates a single long trajectory of the system through phase space, MC typically samples configuration space.

Kikuchi et al. demonstrated, however, that MMC is not restricted to the calculation of equilibrium properties, but can also be used to study dynamic properties. Specifically, they applied the MMC method to the study of Brownian motion of a harmonically bound particle [19]. The same authors further extended the method to study interacting Brownian particles including the effects of hydrodynamic interactions [20].

An different kind of Monte Carlo method is the so-called Kinetic Monte Carlo method (sometimes also called Dynamic Monte Carlo) [21], in which the system is allowed to evolve dynamically from state to state, based on a catalog of transitions and associated rates. Each transition is accepted with a probability proportional to its rate. This, however, assumes that a complete catalog of possible transitions is known in advance (see [22] for an example of the importance of this). Alternatively, a catalog may be built on-the-fly, as proposed by Henkelman et al. [23]. Similar to this technique is the transition state theory (TST)-based MC technique of Liu et al. [24].

In contrast to the processes observed in MD, KMC is not self-consistent, that is, it must be assumed that all possible escape paths from the system's current state can be found. Indeed, if one or several paths are systematically missed, this will corrupt the dynamics of the system [25].

Moreover, often we wish to retain the actual trajectories of the atoms, which is not possible with pure MC techniques. However, in many cases, this is of primordial importance, for instance in the study of particles impinging on a surface. At the same time, it may be desirable to include the effect of long timescale events which bring the system toward equilibrium. For this purpose, MD simulations may be combined with MC simulations.

This paper deals with combining MC with MD simulations. However, it is worth to mention also various other techniques, not based on combining MD with MC, for extending the effective timescale or taking into account

relaxation phenomena [25]. In the following section, we will, therefore, briefly summarize the most prominent techniques that were specifically designed to simulate the dynamical evolution of the system on a longer timescale (i.e., accelerated molecular dynamics). Subsequently, we will present the various possible combinations of coupling MC to MD. Finally, a number of examples of combined MD/MC simulations will be given.

2 Accelerated molecular dynamics techniques

A large number of techniques have been developed for finding saddle points, exploring the free energy landscape of the system and for exploring the potential energy landscape. In the context of accelerating dynamical processes and taking into account long timescale events in the dynamical evolution of a system, we shall here first describe the most prominent techniques for accessing these dynamics. Techniques specifically designed for identifying saddle points and/or reaction paths (such as nudged elastic band [26], the dimer method [27], transition path sampling [28], the activation relaxation technique (ART) [29], forward flux sampling [30], finite temperature string method [31] and milestoning [32], and techniques aimed at sampling the free energy landscape (including thermodynamic integration [33], metadynamics [34], free energy perturbation [35], umbrella sampling [36], adaptive force bias [37] and steered MD [38]), fall outside the scope of this paper.

Prominent among the methods for exploring the atomic scale dynamics of a system, including relaxation and rare events, are temperature-accelerated dynamics (TAD) [39], hyperdynamics [40] and parallel replica [41], all developed by Voter and coworkers. These techniques build on statistical mechanics principles for infrequent event systems, and as such do not make any prior assumptions regarding the atomistic mechanisms. They are designed to simply allow the system to evolve more quickly from state to state than they would in normal MD, provided that the barriers are relatively high compared to kT.

Note that these techniques are not sampling methods, in contrast to (most of) the methods mentioned above. Similar to combined MD/MC simulations in the context of condensed matter systems, they generate a single long state-to-state trajectory.

2.1 Temperature-accelerated dynamics

In TAD, which assumes that harmonic transition state theory (HTST) holds, the simulation is carried out at elevated temperature in order to collect a sequence of escape times from the local energy minimum in which the system

resides. Subsequently, each escape time can be extrapolated to the (lower) temperature of interest, based on the escape time and activation energy as determined from the high temperature simulation. Finally, the transition corresponding to the shortest escape time at the lower temperature is effectively carried out.

Employing this technique, Voter et al. [25] reached a dramatic speed-up factors of 10^7 in the simulation of vapor-deposited growth of a Cu(100) surface at a temperature of 77 K. The simulation conditions corresponded exactly with the experimental conditions of Egelhoff and Jacob [42]. Note, however, that as the boost factor depends on the ratio between the elevated temperature and the lower temperature of interest, much lower factors appear when simulating systems at higher temperatures. Nevertheless, Georgieva et al. [43] recently applied TAD simulations at 500 K to simulate the magnetron sputter deposition of complex oxide Mg–Al–O thin films, extending the typical nanosecond MD timescale to the millisecond range.

2.2 Hyperdynamics

In hyperdynamics, the potential energy surface (PES) of the system is modified by adding a suitable bias potential ΔV. On this modified PES, the system will escape more rapidly from its local state than it would on the original PES. The timescale can be extracted from the value of the bias potential and the MD time required to escape from the state on the modified PES. In contrast to TAD, it only requires TST to hold (instead of HTST), although correlated events are assumed not to occur. In the original hyperdynamics formulation, a Hessian-based bias potential was used [40]. While this approach satisfies the necessary conditions, that is, $\Delta V > 0$ at the potential minimum and $\Delta V = 0$ at the dividing hypersurfaces, it quickly becomes prohibitively expensive with increasing system size as the full $3N$ Hessian needs to be diagonalized in every step.

The main difficulty, therefore, lies in the construction of a suitable and cheap bias potential. Fichthorn et al. [44] developed a so-called bond-boost method, in which the boost potential is derived from the concept of bond breaking events in a solid. Thus, the boost potential in this approach is a function of all nearest-neighbor bond lengths associated with the atoms of interest. Using this technique, these authors studied the diffusion of Cu adatoms, dimers and vacancies on a Cu(001) surface [44]. In these simulations, average boost factors in the range 10^6–10^1 were obtained in the temperature range 230–600 K.

Another very promising way to handle the boost potential problem was proposed by Hamelberg et al. [45].

Their boost potential is defined by functions filling up the energy minima, such that the underlying shape of the unmodified potential energy landscape is retained. At some threshold energy value, the modified potential merges smoothly with the original potential. Combining this boost potential with MC-based system thermalization, Tiwary et al. reached a boost factor of 10^5 for iron lattice diffusion at 285 K.

2.3 Parallel replica

In parallel replica, which is the most exact of the three techniques, a dephased version of the system is replicated on a number of processors. On each of these, the system is allowed to evolve, until a transition is detected on one of the processors. The time accumulated on all processors then corresponds to the advance in simulation time. Parallel replica does not even assume TST to hold. The only requirement is that the infrequent events obey first-order kinetics. Besides this requirement, it is also necessary to dephase the systems on all processors, which typically requires a simulation time of a few ps.

Very recently, Uberuaga employed both TAD and parallel replica simulations to study the formation of fullerene and graphene from carbon nanotube fragments [46]. Using 39 processors, they obtained a boost factor of 28 in the parallel replica simulations, whereas the TAD simulations resulted in boost factors in the range 10–1400 (depending on the exact structure simulated). While the boost factor of parallel replica is typically the lowest of the three methods, it is important to realize that the boost can be trivially increased by increasing the number of processors.

3 Combining MD and MC simulations

3.1 Setting the scene: Monte Carlo simulations

In order to understand Monte Carlo simulations in general and force bias Monte Carlo in particular, it is useful to recall the crucially important condition of detailed balance. This condition can be expressed as

$$W(\mathbf{r}'|\mathbf{r})P(\mathbf{r}) = W(\mathbf{r}|\mathbf{r}')P(\mathbf{r}') \qquad (1)$$

where $P(\mathbf{r})$ is the probability of finding a particle at position $\mathbf{r}$, and $W(\mathbf{r}'|\mathbf{r})$ is the transition probability of the particle to go from position $\mathbf{r}$ to position $\mathbf{r}'$. If P follows a Boltzmann distribution, then

$$\frac{W(\mathbf{r}'|\mathbf{r})}{W(\mathbf{r}|\mathbf{r}')} = \exp(-\beta \Delta U) \qquad \text{with } \beta = \frac{1}{k_B T} \qquad (2)$$

where ΔU is the change in potential energy of the system due to the displacement. W can be rewritten as:

$$W(\mathbf{r}'|\mathbf{r}) = A(\mathbf{r}'|\mathbf{r})T_c(\mathbf{r}'|\mathbf{r}) \quad (3)$$

where T_c $(\mathbf{r}'|\mathbf{r})$ represents the probability distribution of selecting a new position $\mathbf{r}'$ from the old position $\mathbf{r}$, and $A(\mathbf{r}'|\mathbf{r})$ is the probability of accepting this new position. Now, we can define a quantity q as follows:

$$q(\mathbf{r}'|\mathbf{r}) = \frac{T_c(\mathbf{r}|\mathbf{r}')}{T_c(\mathbf{r}'|\mathbf{r})}\exp(-\beta\Delta U) = \frac{T_c'}{T_c}\exp(-\beta\Delta U) \quad (4)$$

Using this quantity q, the condition of detailed balance can now be formulated as

$$A(\mathbf{r}'|\mathbf{r}) = \min[1, q(\mathbf{r}'|\mathbf{r})] \quad (5)$$

Thus, the acceptance of the displacement of a particle from $\mathbf{r}$ to $\mathbf{r}'$ is determined by the associated value of q.

In Metropolis Monte Carlo, T_c is defined as

$$T_c = \begin{cases} c \text{ if } \mathbf{r}' & \in D(\mathbf{r}) \\ 0 \text{ if } \mathbf{r}' & \notin D(\mathbf{r})D(\mathbf{r}) \end{cases} \quad (6)$$

in which $D(\mathbf{r})$ is the displacement domain, and c is a constant. From this, it follows that

$$q = \exp(-\beta\Delta U) \quad (7)$$

From Eqs. 5 and 7, it is immediately clear that when the energy of the system is lowered due to the chosen displacement (i.e., $\Delta U < 0$), this displacement is always accepted, while if the energy increases due to the chosen displacement (i.e., $\Delta U > 0$), the probability of accepting the displacement is equal to $\exp(-\beta\Delta U)$.

3.2 Combined MD/MC algorithms

Various approaches have been proposed to combine MD and MC simulations. Three classes can essentially be distinguished:

1. Mixed MD/MC algorithms, in which some atoms are moved by MD and some by MC;
2. Hybrid MD/MC algorithms, in which the algorithm itself is a combination of MD and MC;
3. Sequential algorithms, in which MD and MC cycles alternate.

Note that most of these algorithms are used to generate a single trajectory, similar to the accelerated molecular dynamics techniques. However, the stochastic MC component does not allow to assign a timescale to the simulation, except in the case of so-called time stamped force bias Monte Carlo (tfMC, see below) [47]. Thus, a comparison in terms of a boost factor with the accelerated dynamics techniques cannot be made.

3.2.1 Mixed MD/MC algorithm

In mixed MD/MC simulations, some of the atoms are moved by the MD method and some of the atoms are moved by the MC method. LaBerge et al. [48] demonstrated that this method rigorously converges to the same equilibrium state as either MC or canonical MD alone. Thus, it was shown that the interruption of the forces produced by the application of the MC moves does not incorrectly bias the evolution of the MD particles. This technique was applied by the above authors to a Lennard-Jones fluid. It was anticipated that this model would be superior to either MD or MC on its own, in systems where some particles are more efficiently sampled by MD (for instance solvent motions), while others are more efficiently sampled by MC (for instance highly correlated motions).

Ribeiro et al. [49] recently used mixed MD/MC simulations of polyalanine systems in water. The MC trials, employing the so-called concerted rotations and angles (CRA) approach of Ulmschneider and Jorgensen [50], were applied to a subset of the peptide atoms; the remaining peptide atoms and the solvent molecules were displaced using MD. It was demonstrated that the mixed MD/MC approach led to a faster formation of the secondary structure, and that the α-helix was formed earlier than in pure MD simulations. It should be noted, however, that both the study of LaBerge et al. and Ribeiro et al. use the mixed MD/MC approach for enhanced sampling of configuration space.

3.2.2 Hybrid algorithms

Whereas in mixed MD/MC simulations, some of the atoms are moved by "pure" MD, and other particles are moved by "pure" MC, it is also possible to construct algorithms in which the displacement itself is determined in part by a deterministic factor and in part by a stochastic factor. In this class, we can further distinguish essentially three techniques: Langevin or stochastic dynamics, hybrid Monte Carlo, and force bias Monte Carlo and related techniques.

Langevin dynamics or stochastic dynamics Langevin dynamics or stochastic dynamics [51] is typically employed for simulating systems in which certain degrees of freedom are omitted. A typical example is the simulation of solvent effects. In this case, one wishes to include the average effect of the solvent on the solute, without explicitly adding all solvent molecules. Stochastic dynamics are based on solving the Langevin equation, in which the total force acting on a particle originates from three contributions: the interaction between the particle and the other particles in the systems (*the systematic force*), a frictional drag component on the particle due to the solvent

(the frictional force), and a random force acting on the particle due to random fluctuations which result from interactions with the solvent (the stochastic force). Thus, the equation to be solved, the Langevin equation, is:

$$m_i \frac{d^2\mathbf{r}_i(t)}{dt^2} = \mathbf{F}_i(\mathbf{r}_i(t)) - \gamma_i \frac{d\mathbf{r}_i(t)}{dt} m_i + \mathbf{R}_i(t) \qquad (8)$$

where $\mathbf{F}_i$ is the systematic force, γ_i is the friction coefficient divided by the mass m of the particle (but it is often simply called the friction coefficient), and $\mathbf{R}_i$ is the stochastic force. Application of Langevin dynamics leads to a canonical distribution.

Langevin dynamics often allow a significant reduction in computation time, due to the fact that there are considerably less particles to be simulated, and also because often longer time steps can be taken relative to MD. Note, however, that Langevin dynamics do not fully simulate the effect of the solvent. Specifically, this method does not account for electrostatic screening, nor for hydrophilic/hydrophobic effects. Furthermore, there is no conservation of energy, and unless the friction coefficient is small, the generated trajectories are not physical [52].

Langevin dynamics are very often used to study biophysical and biochemical systems. For instance, Forray et al. [53] used Langevin dynamics simulations to study the genome packing in bacteriophage. As an all-atom approach is not feasible for such a system, a coarse-graining approach was used, in which the DNA is represented by a wormlike chain of identical beads. Thus, the chemical structure of the DNA double helix is lost. Each Langevin dynamics step corresponded to a time $\Delta t = 12.9$ ps. The structure of the packaged DNA condensate was found to evolve qualitatively according to experimental data. Thus, Langevin dynamics allows to study systems on a larger length scale and on longer timescales than is possible with standard MD, albeit more approximatively.

Hybrid Monte Carlo In MD, all atoms are displaced simultaneously. In MC, however, typically only one or a few particles are displaced at a time, in order to retain a sufficiently high acceptance rate. The moves in MD are limited by the time step, which needs to be sufficiently small in order to conserve the total energy. The moves in MC, on the other hand, are allowed to be large and unphysical. Hybrid Monte Carlo, or Hamiltonian Monte Carlo, was developed by Duane et al. [54] to combine the advantages of both. The idea is to use MD to generate MC trial displacements. Provided that a time-reversible and symplectic algorithm is used, the collective moves thus generated in MD can be accepted or rejected using the standard MMC criterion. The end result is that trials move across the sample space in larger steps, and because of the Hamiltonian evolution of the system between states, the correlation between successive states is reduced. However,

as pointed out by Frenkel and Smit [1], the performance of hybrid MC is not always dramatically better than that of the corresponding MD, although hybrid MC might be advantageous for systems that are not too large.

This technique is most often used in lattice quantum chromodynamics (QCD) simulations. Mehlig et al. [55] demonstrated its use by simulating Lennard-Jonesium as an example of a condensed matter system. Similarly, Clamp et al. [56] simulated a 2D Lennard-Jones fluid using both MD and hybrid MC and found that hybrid MC is more ergodic and samples phase space more efficiently than MD. A more realistic system was studied by Brotz et al. [57], employed hybrid MC to calculate the phase diagram of silicon.

Force bias Monte Carlo and related techniques Several variants of force bias Monte Carlo (fbMC) simulations have been presented in the literature. Essentially, the goal of these algorithms is to have a higher acceptance probability of the atomic displacements relative to MMC, and thus to allow the system to evolve to equilibrium more quickly. The original fbMC method was introduced by Pangali et al. [59, 58]. In the original version, an acceptance criterion was used to accept or reject a new configuration. In later versions by Dereli [60], Mezei [61] and Timonova [62], a uniform acceptance was employed. Recently, detailed balance in these uniform acceptance algorithms was formally demonstrated by Neyts et al. [63].

In fbMC, the possible displacements are *not* chosen randomly in the domain $D(\mathbf{r})$, but are dependent on the force acting on the particle, in contrast to the MMC method. The transition matrix is now written as (in the x-coordinate):

$$T_{c,x} = \begin{cases} K_x^{-1} \exp(\lambda\beta F_x\delta_x) & \text{if } x' \in D(x) \\ 0 & \text{if } x' \notin D(x) \end{cases} \qquad (9)$$

In this expression, the displacement δ_x is given by $\delta_x = x' - x$, F_x is the x-component of the force at position x, K_x^{-1} is a normalization constant, and λ is a (in principle) arbitrary parameter. Analogous expressions appear for the components in the other directions.

Thus, from Eq. 9, it is clear that displacements in the direction of the force are more probable than displacements against the force. As a result, considerably less displacements need to be rejected compared to the Metropolis algorithm. The obvious downside is that the force needs to be calculated.

If the domain $D(\mathbf{r})$ corresponds to a cube centered around $\mathbf{r} = (x, y, z)$ and sides $2\Delta \times 2\Delta \times 2\Delta$, then each displacement in a direction v is limited as:

$$-\Delta \le \delta_v \le \Delta \qquad (10)$$

and the displacement can be written as

$$\mathbf{r}' = \mathbf{r} + \xi \cdot \Delta \qquad (11)$$

Each component $\xi_v \in [-1, 1]$ from the vector $\xi = \{\xi_x, \xi_y, \xi_z\}$ can be computed based on a random number $\eta \in [0, 1]$ as

$$\xi_v = \frac{1}{\gamma_v} \ln \left[\eta \left(e^{|\gamma_v|} - e^{-|\gamma_v|} \right) + e^{-|\gamma_v|} \right] \tag{12}$$

in which

$$\gamma_v = \lambda \beta F_v \Delta \tag{13}$$

Just as in the case of MMC, all displacements need to be accepted or rejected, based on the value of q and thus of A. Mezei et al. [61] used this technique to simulate a DNA-octamer duplex and Na^+ions solvated by water molecules employing the AMBER force field.

Dereli [60] proposed to use $\lambda = 1/2$ and accept all displacements, instead of using q to accept or reject displacements. Somewhat confusingly, Dereli termed this technique *Dynamic Monte Carlo*. Recently, Timonova et al. thoroughly reviewed the method and termed it *uniform acceptance force bias Monte Carlo* [62]. These authors performed a number of tests to investigate under which conditions reliable results can be expected. The authors recommended to use a realistic value for the temperature parameter, although it should be treated carefully, especially when using large maximum displacements. From their simulations, it seems that a value for the maximum allowed displacement in the range $\Delta/2 = 0.06R_{eq} - 0.15R_{eq}$, where R_{eq} is the equilibrium bond length, is appropriate for temperatures at or above room temperature for silicon. The exact value is dependent on the desired accuracy and speed of the simulation.

Very recently, a formal proof was presented by Neyts et al. [63] that this uniform acceptance formulation using $\lambda = 1/2$ complies with detailed balance, provided that the domain D, and thus the maximum allowed displacement, is chosen sufficiently small. Note that this value is dependent on both the exact potential, as well as on the temperature. The higher the temperature, the larger the maximum displacement can be chosen without violating detailed balance.

A novel version of the uniform acceptance algorithm was recently published by Mees et al. [47]. In this version, which was termed *time stamped force bias Monte Carlo* (tfMC), the conditional probability for a displacement in the x-direction is given by:

$$P_{c,x}(\xi_x) = \begin{cases} \frac{e^{\gamma_x(2\xi_x+1)} - e^{-\gamma_x}}{e^{\gamma_x} - e^{-\gamma_x}} & \xi_x \in [-1, 0[\\ \frac{e^{\gamma_x} - e^{\gamma_x(2\xi_x-1)}}{e^{\gamma_x} - e^{-\gamma_x}} & \xi_x \in]0, 1] \end{cases}. \tag{14}$$

Again, analogous expressions appear for the other directions. In practice, a pair of random numbers (ξ_v, P_v) is generated for each direction v, with $\xi_v \in [-1, 1]$ and $P_v \in [0, 1]$ for all atoms. If $P_{c,v}(\xi_v) > P_v$, the displacement of

the atom is accepted and its new position is $r_{v,new} = r_{v,old} + \Delta \xi_v$. Else, if $P_{c,v}(\xi_v) < P_v$, a new random pair (ξ_v, P_v) is generated and its acceptance is reevaluated.

From Eq. 12, it is clear that in fbMC, the displacement of the particles is based on both a deterministic component, that is, the force, and a stochastic component, that is, a random number(s). At low temperature, the deterministic component dominates, and all displacements are essentially in the direction of the force. At high temperature, on the other hand, all displacements will be essentially fully random.

Importantly, an expression for the statistical time per MC step was derived from this algorithm:

$$\langle \Delta t \rangle = \frac{\Delta}{3} \cdot \sqrt{\frac{\pi m_{\min}}{2k_B T}} \tag{15}$$

in which $m_{\min}$ is the mass of the lightest element present in the simulation. In contrast to MMC, this allows to assign a timescale to the MC simulation. From their tests, the authors concluded that time steps between about 2 fs and 50 fs per tfMC step can be obtained. This represents a speed-up relative to MD by a factor of about 2–50 [47]. While this value may seem low compared to the very high boost factors that may be obtained in accelerated dynamics as described above, it should be realized that tfMC in contrast to accelerated dynamics is not limited to infrequent event systems, and it does not require (H)TST to hold. Thus, while the speedup is indeed limited, the method can be considered to have a wider applicability.

Very similar to these force bias Monte Carlo algorithms is the *Smart Monte Carlo* technique by Rossky et al. [64]. This technique also requires the forces acting on the moving atom to be calculated. Also, the displacement is determined by two components, that is, the force, which acts as the deterministic component, and a random vector $\delta \mathbf{r}_i^R$. The displacement is then written as

$$\delta \mathbf{r}_i = \frac{A \mathbf{F}_i}{k_B T} + \delta \mathbf{r}_i^R \tag{16}$$

where $\mathbf{F}_i$ is the force acting on particle i and A is a parameter. The random vector $\delta \mathbf{r}_i^R$ is chosen from a normal distribution with zero mean and variance $2A$.

In contrast to the fbMC methods, the smart Monte Carlo method does not impose a limit on the maximum displacement of the particles. This obviously implies that in this case, acceptance or rejectance must be verified by calculating q (cfr. Eq. 4 above).

3.2.3 Sequential algorithms: alternating MD and MC

Many authors have combined MD and MC by simply allowing one technique to alternate with the other technique. In most cases, one technique is applied to all atoms

for a predetermined number of steps. The resulting output is subsequently used as input to the other technique, which is also run for a predetermined number of steps. Again, the resulting output is then used as input to the first technique and the cycle repeats.

The underlying idea is that MD can be used to simulate fast processes, for instance the impingement of reactive species on a surface and the chemical bonding to the surface, while the subsequent MC steps take into account the longer timescale thermal relaxation processes, as schematically depicted in Fig. 1. This technique has for instance been applied to the fast equilibration of complex systems such as lipid-cholesterol lipid bilayers and fully hydrated dioleyl and palmitoyl-oleyl phosphatidylcholine lipid bilayers [65, 66], but it is equally suited for simulating for instance deposition processes. Indeed, while in some cases deposition and growth may be successfully simulated using MD alone (see for instance [6, 67], longer timescale processes are very often a critical factor in determining the final thin film properties.

Taguchi et al. [68, 69] applied this technique to model the reactive sputter deposition of thin SiO_2 films and the effect of Ar bombardment on the SiO_2 deposition process. In this particular case, it was found that simulating the deposition process by MD alone resulted in films with a much lower density that those typically obtained from experiments under similar conditions. Applying the sequential MD/MC approach, amorphous SiO_2 films with properties consistent with experiments were obtained.

A somewhat different version of this idea was presented by Tavazza et al. [70]. In their approach, collective moves are added to the standard single-atom moves in the MC method. When an atom or several atoms are displaced by MC, the local environment is first relaxed using a small number of MD steps at constant temperature. Only after this relaxation process the displacement is evaluated and accepted or rejected using the standard Boltzmann criterion. Thus, in their approach, the MD displacements are effectively used as trial displacements for the MC simulation, and as such this idea corresponds to the hybrid MC concept (see above, Sect. 3.2.2)

Yet another version of the same idea was presented by Tiwary and van de Walle [71]. In their approach, the system evolves according to standard MD when the potential energy is above some threshold, whereas it evolves according to MMC when the potential energy falls below

Fig. 1 Schematic representation of the alternating MD/MC approach

this threshold. The MC part takes care of the relaxation of the system, whereas the MD part allows the system to explore the high energy region of phase space in which the infrequent events occur. As there are no velocities in the MC part, the atomic velocities in the MD part are initiated from a truncated Maxwell-Boltzmann distribution at the temperature of interest such that $\mathbf{v}_i \cdot \mathbf{f}_i > 0$ where $\mathbf{v}_i$ is the chosen atomic velocity, and $\mathbf{f}_i$ is the force acting on the atom. In parallel to the MC run intended to relax the system, a second MC run is launched to estimate the time the system should have spent in the potential well.

Tiwary et al. [71] applied this algorithm to the vacancy-mediated diffusion in iron and the plasticity and deformation of Au nanopillars at realistic strain rates. In both cases, good agreement with the literature is found, and for the diffusion studies, an impressive boost factor of 10^5 was obtained, demonstrating the usefulness of their technique in the field of condensed matter simulations.

3.2.4 Sequential algorithms: alternating hybrid algorithms

It is of course also possible to combine MD with fbMC, or fbMC with MMC, etc. Various examples can be found in the literature.

Timonova et al. [62] explored two rather similar versions of combining MD and fbMC, which they termed "UFMC+" and "UFMC++," both aiming at bringing the system back to thermal equilibrium and reduce the unphysical spread in atomic potential energies produced by the fbMC algorithm. As pointed out by these authors, this starts by assigning velocities to the atoms, which are absent in the fbMC algorithm. In their UFMC+ simulations, zero velocities were attributed to all atoms, followed by a short NVT MD run at the temperature corresponding to the fbMC temperature. In the UFMC++ version, all atoms were again given zero velocities, and followed by a short constant temperature MD run, but this time with the thermostat set to 0 K. This effectively results in a system quenched to 0 K. The authors found that in both cases, equilibrium was reached in about 1.5 ps. The UFMC+ simulations were used to study the solid–liquid phase transition of Si.

Grein et al. [72] employed a fbMC/MMC technique for simulation of a deposition process. Similar to Taguchi et al. (who used a MD/MMC approach instead of fbMC/MMC [68, 69], these authors used fbMC to follow the actual deposition process and MMC for the subsequent equilibration. The goal was to describe the initial nucleation and growth of Ge epitaxially depositing on Si(001) surfaces. Interestingly, they used a maximum displacement length of 0.5 Å in their fbMC simulations while accepting all displacements. This displacement length is a factor of 100 or more larger than a typical displacement in MD.

While such a large step size must certainly violate detailed balance (see [63]), the authors nevertheless obtained results which seem physically reasonable. It should be noted that such large displacements can be used successfully if an acceptance criterion is used, as was done in the original formulation by Pangali et al. [58, 59].

4 Examples of combined MD/MC

In this section, we will review three representative examples of the techniques described above in the context of reactive condensed matter simulations, taken from our own research efforts: Cu surface diffusion by fbMC, (ultra) nanocrystalline diamond (UNCD) growth using sequential MD/MMC and carbon nanotube (CNT) growth using sequential MD/fbMC.

4.1 Hybrid algorithms: Cu surface diffusion by tfMC

As a first basic example, we consider the diffusion of a Cu adatom on a solid Cu (001) surface, as simulated by tfMC [47]. The Cu–Cu interaction was described by the standard embedded atom method potential. The diffusion coefficient was determined directly from the calculated trajectories, and the rate constant was calculated from the Arrhenius equation. The tfMC simulations were carried out using $\Delta = 0.10$ Å, corresponding to an average MC time step between 7.8 and 10 fs, in the temperature range 550–900 K, and compared with both MD simulations as well as with the literature. The dynamics of the adatom diffusion process as determined from the tfMC algorithm are shown in Fig. 2. It was found that tfMC correctly reproduces the different diffusion mechanisms as observed in the MD simulations. Also, the activation barrier as determined from
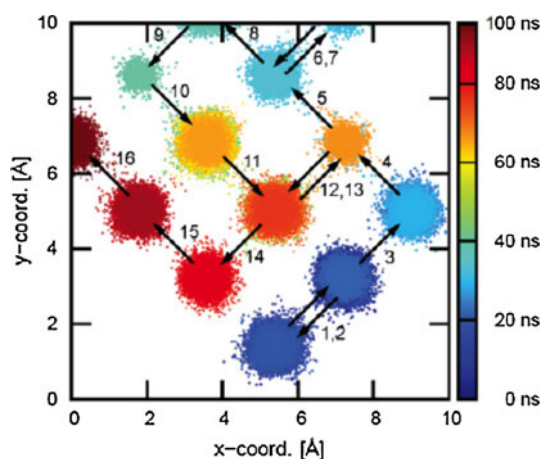

Fig. 2 Illustration of the Cu adatom diffusion dynamics as observed in tfMC simulations. Reproduced with permission by the American Physical Society from [47]

tfMC, 0.48 eV, is in close agreement with the literature values (0.43–0.51 eV). Interestingly, however, the frequency factor found from the tfMC simulations, 14.7 THz, is in much closer agreement with the literature values (7.5–35.8 THz) than the MD value (52.5 THz). This demonstrates that tfMC is indeed capable of correctly reproducing the atomic dynamics of the system while significantly increasing the timescale that can be reached.

4.2 Alternating MD and MC: (U)NCD growth by MD/MMC

As mentioned in the previous sections, the combination of MC with MD may provide a means to take into account events that occur on timescales that are beyond the reach of pure MD simulations. Thus, we performed a number of hybrid MD/MMC simulations relevant for NCD and UNCD growth, based on the Brenner potential [73, 74, 75]. In an attempt to minimize the computational effort, we combined MD with MMC, introducing two additional criteria, in addition to the standard Metropolis acceptance criterion [74]. In this implementation, a criterion is used to select which atoms are displaced in the MMC (in contrast to moving all the atoms), as well as a criterion deciding after how many steps the MMC is stopped. We found that the MD/MMC algorithm predicts the same processes to occur as pure MD while allowing a speedup of typically one order of magnitude. As a simple example of the application of this technique, Fig. 3 shows the formation of a new diamond 6-ring starting from a previously adsorbed C-atom and C_2H_2 molecule.

These kind of simulations again provide atomic scale insights into the mechanisms, while the resulting structures correspond to the experiment. For instance, the effect of the prolonged application of a bias on the nucleation was investigated by both MD/MMC simulations and experiments [73]. In agreement with the experiment, an exponential increase in the growth rate was observed at high bias voltages. Complementary to the experimental data, it was found that this is caused by the increased flux of reactive particles toward the substrate. Furthermore, it was found that the growing film is activated by the formation of reactive sites when a sufficiently high bias is applied. Also in agreement with the literature, an enhanced formation of long-range order in the films was obtained by the application of a bias up to 100 V. Applying bias voltages above 100 V, diamond crystallites could not be formed, again in agreement with experimental findings.

4.3 Alternating hybrid algorithms: CNT growth by MD/fbMC

Carbon nanotubes continue to attract a lot of research attention because of their extraordinary mechanical, optical
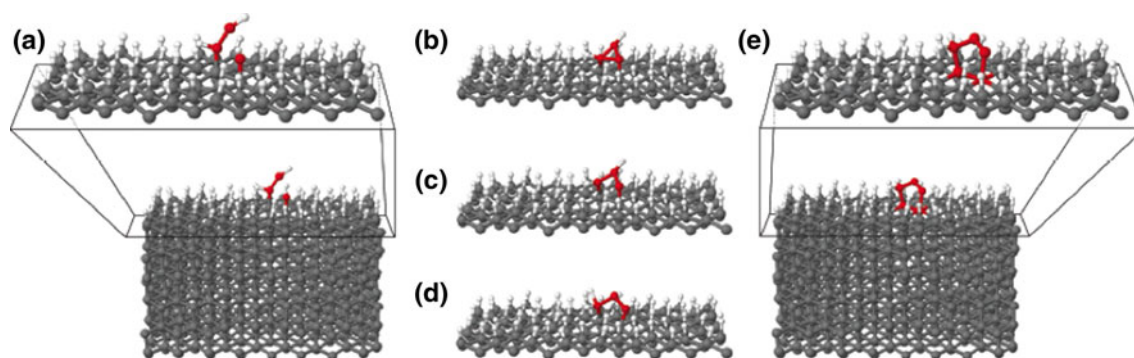
Fig. 3 Formation of a new diamond 6-ring from an adsorbed C-atom and adsorbed C_2H_2 molecule as observed in a MD/MMC simulation. **a** The initial configuration, **b–d** intermediate states and **e** the final state. The *red* atoms indicate the carbon atoms involved in the formation of the new diamond 6-ring. Reproduced from [74] with permission from the Royal Society of Chemistry

and electronic properties. However, these properties are directly determined by their precise structure, thus necessitating very accurate control over the growth process. In this case, atomistic simulations may provide the atomic scale insight needed to understand how the growth process might be controlled, and why specific structures are formed for a given growth condition.

One very important factor during the growth is the phase state of the nanocatalyst. Thus, we performed MD/fbMC simulations, employing the Shibuta potential, to determine the phase state of various Ni-nanoparticles as a function of size and temperature [76]. In this work, the thermalization was carried out using combined MD/fbMC simulations. Analysis of the radial distribution of the atomic Lindemann index revealed that that for the smallest clusters, a dynamic coexistence process occurs. As illustrated in Fig. 4, surface melting is observed for the larger particles. In all cases, a significant depression of the melting temperature relative to the bulk was observed, due to the Gibbs–Thomson effect, in agreement with the literature [77–79].

Subsequently, a number of combined MD/fbMC simulations were performed to study the growth of carbon nanotubes based on the ReaxFF potential to gain an atomic scale understanding in the actual growth process [80–82]. In these simulations, rather conservative values for $\Delta/2 = 0.085 R_{eq}$ [80] and $\Delta/2 = 0.07 R_{eq}$ [81, 82] in the fbMC were chosen. The temperature was set to 1,000 K, corresponding to a typical experimental growth temperature. After each MC cycle, new random velocities were assigned to all atoms, and the simulation was continued with constant temperature MD. Similar to Grein et al., the impact and deposition of atoms (in this case C-atoms) on the substrate (in this case a Ni-nanocluster) were followed by MD, and the subsequent relaxation by fbMC. It was found that the fbMC method results in healing of the carbon network that is formed by the continuous addition of carbon atoms—a process in which high barriers must be overcome. An example of this healing mechanism as
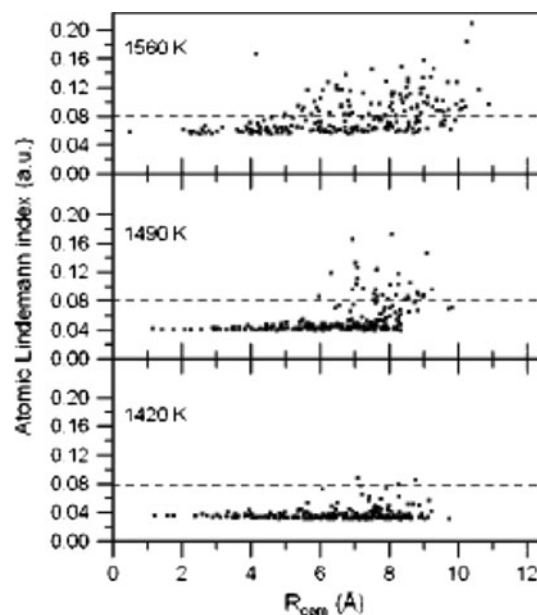

Fig. 4 Calculated radial distribution of the atomic Lindemann index for a Ni_{244} cluster, for various temperatures, revealing a surface melting mechanism. Reproduced from [15] with permission from the American Chemical Society

observed in the fbMC is shown in Fig. 5. This then finally leads to CNTs with very few defects, as illustrated in Fig. 6, in contrast to what is typically observed in pure MD growth simulations. Both metallic tubes [81] as well as semi-conducting tubes [80] could be obtained. Furthermore, we also observed that the chirality of the tube may change in the initial nucleation stage. It was found that this is due to the incorporation of asymmetric defects, such as so-called 5–7 defects [81]. Thus, these MD/fbMC simulations allow to gain an understanding of how the longer timescale events may influence the growth process.

In another study, we used MD/fbMC simulations to investigate how an electric field may influence the growth process. In agreement with the experiment [83, 84], SWNT
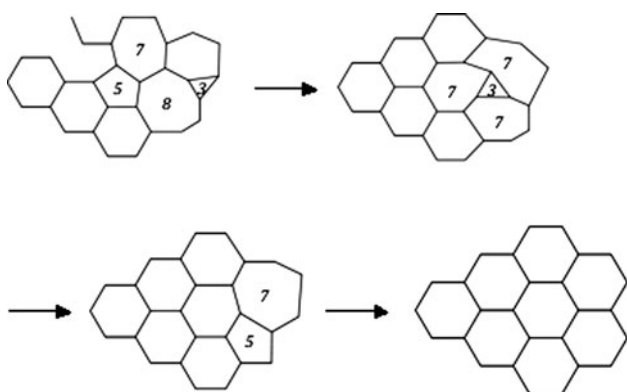
Fig. 5 Observed healing mechanism of the growing carbon network during CNT growth. Reproduced from [81] with the permission of the American Chemical Society

Fig. 6 Simulated SWNT growth based on the MD/fbMC technique, resulting in a SWNT with (7, 7) chirality. Reproduced from [81] with permission from the American Chemical Society
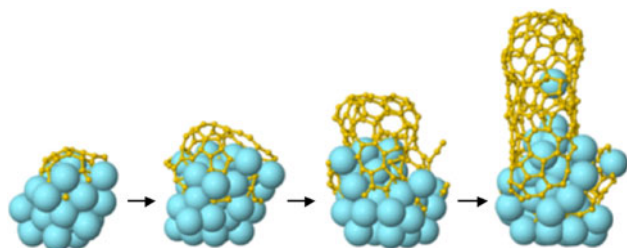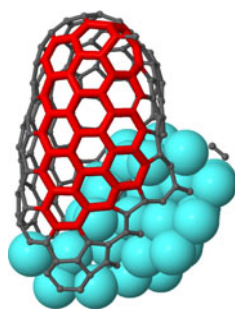

Fig. 7 MD/fbMC simulation of vertically aligned SWNT growth by applying an electric field of 700 kV/cm [82]

alignment was observed if a (sufficiently strong) electric field was applied. This is shown in Fig. 7 for an electric field value of 700 kV/cm. These simulations shed a new light on the underlying mechanism: we found that the electric field is primarily acting on the polar Ni–C bonds, at the interface between the nickel nanocluster and the growing SWNT. Thus, as at this interface the C-atoms are slightly negative, while the Ni-atoms are slightly positive, the carbon atoms experience both an oriented force, pulling them toward the tip of the cluster, but are also subject to random thermal diffusion. If the electric field is sufficiently strong, the directed migration dominates the random diffusion, an a vertically aligned SWNT emerges. Thus, these

simulations directly provide information about the relevant processes complementary to the experiment.

5 Conclusion

In this contribution, we have presented a brief summary of the main accelerated molecular dynamics techniques as well as more a elaborate description of the various techniques for combining MD simulations with MC simulations, as an alternative to accelerated molecular dynamics simulations for generating long system trajectories. Using examples from the literature, it is shown that combined MD/MC simulations may provide a dynamic picture of a reactive system, including relaxation events which take place on timescales typically beyond the reach of pure MD. Essentially, we can distinguish between algorithms in which some atoms are moved by MD and some by MC (*combined MD/MC method*), algorithms in which the atomic displacement prescription is in part deterministic and in part stochastic (*hybrid MD/MC method*), and algorithm in which MD cycles alternate with MC cycles (*sequential MD/MC method*).

Three representative examples from our own research efforts were shown to demonstrate the applicability of MD/MC simulations, viz. Cu adatom diffusion, UNCD growth and CNT growth.

In addition to their ease of implementation and their general applicability make these methods very attractive for studying systems in which processes beyond the reach of standard MD are important.

References

1. Frenkel D, Smit B (2001) Understanding molecular simulation: from algorithms to applications. Academic Press, London
2. Cooke DJ, Elliott JA (2007) Atomistic simulations of calcite nanoparticles and their interaction with water. J Chem Phys 127(10). Art no 104706
3. Khalilov U, Pourtois G, van Duin ACT, Neyts EC (2012) self-limiting oxidation in small-diameter Si nanowires. Chem Mater 24(11):2141–2147
4. Lu Y, Cheng H, Chen M (2012) A molecular dynamics examination of the relationship between self-diffusion and viscosity in liquid metals. J Chem Phys 136(21). Art no 214505
5. Matsukuma M, Hamaguchi S (2008) Molecular dynamics simulation of microcrystalline Si deposition processes by silane plasmas. Thin Solid Films 516(11):3443–3448
6. Neyts E, Bogaerts A, Gijbels R, Benedikt J, Van De Sanden M (2004) Molecular dynamics simulations for the growth of diamond-like carbon films from low kinetic energy species. Diam Relat Mater13(10):1873–1881
7. Faccioli P, Lonardi A, Orland H (2010) Dominant reaction pathways in protein folding: a direct validation against molecular dynamics simulations. J Chem Phys 133(4). Art no 045104

8. Rauf S, Sparks T, Ventzek PLG, Smirnov VV, Stengach AV, Gaynullin KG, Pavlovsky VA (2007) A molecular dynamics investigation of fluorocarbon based layer-by-layer etching of silicon and SiO2. J Appl Phys 101(3). Art no 033308

9. Gou F, Neyts E, Eckert M, Tinck S, Bogaerts A (2010) Molecular dynamics simulations of Cl+ etching on a Si(100) surface. J Appl Phys 107(11):113305

10. Postawa Z, Czerwinski B, Szewczyk M, Smiley E, Winograd N, Garrison B (2003) Enhancement of sputtering yields due to C-60 versus Ga bombardment of Ag{111} as explored by molecular dynamics simulations. Anal Chem 75(17):4402–4407

11. Shen XJ, Xiao Y, Dong W, Yan XH, Busnengo HF (2012) Molecular dynamics simulations based on reactive force-fields for surface chemical reactions. Comput Theor Chem 990: 152–158

12. Servantie J, Gaspard P (2003) Methods of calculation of a friction coefficient: application to nanotubes. Phys Rev Lett 91(18). Art no 185503

13. Thaulow C, Sen D, Buehler MJ (2011) Atomistic study of the effect of crack tip ledges on the nucleation of dislocations in silicon single crystals at elevated temperature. Mater Sci Eng A Struct Mater Prop Microstruct Process 528(13–14):4357–4364

14. Shibuta Y (2012) Phase transition of metal nanowires confined in a low-dimensional nanospace. Chem Phys Lett 532:84–89

15. Neyts EC, Bogaerts A (2009) Numerical study of the size-dependent melting mechanisms of nickel nanoclusters. J Phys Chem C 113(7):2771–2776

16. Dongare AM, Rajendran AM, LaMattina B, Zikry MA, Brenner DW (2009) Atomic scale studies of spall behavior in nanocrystalline Cu. J Appl Phys 108(11):113518

17. Shaw DE, Maragakis P, Lindorff-Larsen K, Piana S, Dror RO, Eastwood MP, Bank JA, Jumper JM, Salmon JK, Shan Y, Wriggers W (2010) Atomic-level characterization of the structural dynamics of proteins. Science 330(6002):341–346

18. Metropolis N, Rosenbluth AW, Rosenbluth MN, Teller AH, Teller E (1953) Equation of state calculations by fast computing machines. J Chem Phys 21(6):1087

19. Kikuchi K, Yoshida M, Maekawa T, Watanabe H (1991) Metropolis Monte–Carlo method as a numerical technique to solve the Fokker-Planck equation. Chem Phys Lett 185(3–4): 335–338

20. Kikuchi K, Yoshida M, Maekawa T, Watanabe H (1992) Metropolis Monte-Carlo method for Brownian dynamics simulation generalized to include hydrodynamic interactions. Chem Phys Lett 196(1–2):57–61

21. Bortz AB, Kalos MH, Leibowitz JL (1975) A new algorithm for Monte Carlo simulation of Ising spin systems. J Comput Phys 17:10–18

22. Netto A, Frenklach M (2005) Kinetic Monte Carlo simulations of CVD diamond growth—interlay among growth, etching, and migration. Diam Relat Mater 14(10):1630–1646

23. Henkelman G, Jonsson H (2001) Long time scale kinetic Monte Carlo simulations without lattice approximation and predefined event table. J Chem Phys 115(21):9657–9666

24. Liu YH, Neyts E, Bogaerts A (2006) Monte Carlo method for simulations of adsorbed atom diffusion on a surface. Diam Relat Mater 15(10):1629–1635

25. Voter A, Montalenti F, Germann T (2002) Extending the time scale in atomistic simulation of materials. Ann Rev Mater Res 32:321–346

26. Jonsson H, Mills G, Jacobsen KW (1998) Nudged elastic band method for finding minimum energy paths of transitions. In: Berne BJ, Ciccotti G, Coker DF (ed) Classical and quantum dynamics in condensed phase simulations. World Scientific, Singapore

27. Henkelman G, Jonsson H (1999) A dimer method for finding saddle points on high dimensional potential surfaces using only first derivatives. J Chem Phys 111:7010–7022

28. Dellago C, Bolhuis PG, Csajka FS, Chandler D (1998) Transition path sampling and the calculation of rate constants. J Chem Phys 108(5):1964–1977

29. Barkema GT, Mousseau N (1996) Event-based relaxation of continuous disordered systems. Phys Rev Lett 77(21): 4358–4361

30. Allen RJ, Warren PB, ten Wolde PR (2005) Sampling rare switching events in biochemical networks. Phys Rev Lett 94: 018104

31. Ren WE, Vanden-Eijnden E (2005) Finite temperature string method for the study of rare events. J Phys Chem B 109:6668

32. Faradijan AK, Elber R (2004) Computing time scales from reaction coordinates by milestoning. J Chem Phys 120:10880–10889

33. Tironi IG, van Gunsteren WF (1994) A molecular-dynamics simulation study of chloroform. Mol Phys 83(2): 381–403

34. Laio A, Parrinello M (2002) Escaping free-energy minima. Proc Natl Acad Sci USA 99(20):12562–12566

35. Zwanzig RW (1954) High temperature equation of state by a perturbation method. I. Nonpolar gases. J Chem Phys 22:1420–1426

36. Torrie GM, Valleau JP (1977) Nonphysical sampling distributions in Monte Carlo free-energy estimation: umbrella sampling. J Comput Phys 22(2):187–199

37. Darve E, Pohorille A (2001) Calculating free energies using average force. J Chem Phys 115: 9169–9183

38. Leech J, Prins J, Hermans J (1996) SMD: Visual steering of molecular dynamics for protein design. IEEE Comput Sci Eng 3:38–45

39. Sorensen M, Voter A (2000) Temperature-accelerated dynamics for simulation of infrequent events. J Chem Phys 112(21): 9599–9606

40. Voter A (1997) Hyperdynamics: accelerated molecular dynamics of infrequent events. Phys Rev Lett 78(20):3908–3911

41. Voter A (1998) Parallel replica method for dynamics of infrequent events. Phys Rev B Condens Matter 57(22): 13985–13988

42. Egelhoff WF, Jacob I (1998) Reflection high-energy electron-diffraction (RHEED) oscillations at 77 K. Phys Rev Lett 62(8): 921–924

43. Georgieva V, Voter AF, Bogaerts A (2011) Understanding the surface diffusion processes during magnetron sputter-deposition of complex oxide Mg-Al-O thin films. Cryst Growth Des 11(6): 2553–2558

44. Fichthorn KA, Miron RA, Wang YS, Tiwary Y (2009) Accelerated molecular dynamics simulation of thin-film growth with the bond-boost method. J Phys Condens Matter 21(8):084212

45. Hamelberg D, Mongan J, McCammon JA (2004) Accelerated molecular dynamics: a promising and efficient simulation method for biomolecules. J Chem Phys 120(24): 11919–11929

46. Uberuaga BP, Stuart SJ, Windl W, Masquelier MP, Voter AF (2012) Fullerene and graphene formation from carbon nanotube fragments. Comput Theor Chem 987(SI):115–121

47. Mees MJ, Pourtois G, Neyts EC, Thijsse BJ, Stesmans A (2012) Uniform-acceptance force-bias Monte Carlo method with time scale to study solid-state diffusion. Phys Rev B 85(13):134301

48. Laberge L, Tully J (2000) A rigorous procedure for combining molecular dynamics and Monte Carlo simulation algorithms. Chem Phys 260(1-2):183–191

49. Ribeiro AAST, de Alencastro RB (2012) Mixed Monte Carlo/molecular dynamics simulations in explicit solvent. J Comput Chem 33(8):901–905

50. Ulmschneider JP, Jorgensen WL (2003) Monte Carlo backbone sampling for polypeptides with variable bond angles and dihedral angles using concerted rotations and a Gaussian bias. J Chem Phys 118(9):4261–4271

51. Leach AR (2001) Molecular modelling: principles and applications. Prentice Hall, Essex

52. Bussi G, Donadio D, Parrinello M (2007) Canonical sampling through velocity rescaling. J Chem Phys 126(1):014101

53. Forray C, Muthukumar M (2006) Langevin dynamics simulations of genome packing in bacteriophage. Biophys J 91:25–41

54. Duane S, Kennedy A, Pendleton B, Roweth D (1987) Hybrid Monte-Carlo. Phys Lett B 195(2):216–222

55. Mehlig B, Heermann D, Forrest B (1992) Hybrid Monte-Carlo method for condensed-matter systems. Phys Rev B 45(2): 679–685

56. Clamp ME, Baker PG, Stirling CJ, Brass A (1994) Hybrid Monte-Carlo—an efficient algorithm for condensed matter simulation. J Comput Chem 15(8):838–846

57. Brotz FA, Depablo JJ (1994) Hybrid Monte-Carlo simulation of silica. Chem Eng Sci 49(17):3015–3031

58. Pangali C, Rao M, Berne B (1978) Novel Monte-Carlo scheme for simulating water and aqueous-solutions. Chem Phys Lett 55(3):413–417

59. Rao M, Pangali C, Berne B (1979) Force bias Monte-Carlo simulation of water—methodology, optimization and comparison with molecular-dynamics. Mol Phys 37(6):1773–1798

60. Dereli G (1992) Stillinger-Weber type potentials in Monte-Carlo simulation of amorphous-silicon. Mol Simul 8(6):351–360

61. Mezei M (1991) Distance-scaled force biased Monte Carlo simulation for solutions containing a strongly interacting solute. Mol Simul 5:405–408

62. Timonova M, Groenewegen J, Thijsse BJ (2010) Modeling diffusion and phase transitions by a uniform-acceptance force-bias Monte Carlo method. Phys Rev B 81(14):144107

63. Neyts EC, Thijsse BJ, Mees MJ, Bal KM, Pourtois G (2012) Establishing uniform acceptance in force biased Monte Carlo simulations. J Chem Theory Comput 8: 1865–1869

64. Rossky P, Doll J, Friedman H (1978) Brownian dynamics as smart Monte-Carlo simulation. J Chem Phys 69(10): 4628–4633

65. Chiu S, Jakobsson E, Scott H (2001) Combined Monte Carlo and molecular dynamics simulation of hydrated lipid-cholesterol lipid bilayers at low cholesterol concentration. Biophys J 80(3): 1104–1114

66. Chiu S, Jakobsson E, Subramaniam S, Scott H (1999) Combined Monte Carlo and molecular dynamics simulation of fully hydrated dioleyl and palmitoyl-oleyl phosphatidylcholine lipid bilayers. Biophys J 77(5):2462–2469

67. Jager HU, Belov AY (2003) ta-C deposition simulations: film properties and time-resolved dynamics of film formation. Phys Rev B 68(2):024201

68. Taguchi M, Hamaguchi S (2006) Molecular dynamics study on Ar ion bombardment effects in amorphous Sio2 deposition processes. J Appl Phys 100(12):123305

69. Taguchi M, Hamaguchi S (2007) Md simulations of amorphous Sio2 thin film formation in reactive sputtering deposition processes. Thin Solid Films 515(12):4879–4882

70. Tavazza F, Nurminen L, Landau D, Kuronen A, Kaski K (2004) Hybrid Monte Carlo-molecular dynamics algorithm for the study of islands and step edges on semiconductor surfaces: application to Si/Si(001). Phys Rev E 70(3, Part 2): 036701

71. Tiwary P, van de Walle A (2011) Hybrid deterministic and stochastic approach for efficient atomistic simulations at long time scales. Phys Rev B 84(10):100301

72. Grein C, Benedek R, Delarubia T (1996) Epitaxial growth simulation employing a combined molecular dynamics and Monte Carlo approach. Comput Mater Sci 6(2):123–126

73. Eckert M, Mortet V, Zhang L, Neyts E, Verbeeck J, Haenen K, Bogaerts A (2011) Theoretical investigation of grain size tuning during prolonged bias-enhanced nucleation. Chem Mater 23(6): 1414–1423

74. Eckert M, Neyts E, Bogaerts A (2009) Modeling adatom surface processes during crystal growth: a new implementation of the metropolis Monte Carlo algorithm. CrystEngComm 11(8):1597–1608

75. Eckert M, Neyts E, Bogaerts A (2010) Insights into the growth of (ultra) nanocrystalline diamond by combined molecular dynamics and Monte Carlo simulations. Cryst Growth Design 10(7): 3005–3021

76. Neyts EC, Khalilov U, Pourtois G, Van Duin ACT (2011) Hyperthermal oxygen interacting with silicon surfaces: adsorption, implantation, and damage creation. J Phys Chem C 115(11): 4818–4823

77. Buffat P, Borel J (1976) Size effect on melting temperature of gold particles. Phys Rev A 13(6):2287–2298

78. Jiang A, Awasthi N, Kolmogorov AN, Setyawan W, Borjesson A, Bolton K, Harutyunyan AR, Curtarolo S (2007) Theoretical study of the thermal behavior of free and alumina-supported Fe-C nanoparticles. Phys Rev B 75(20):205426

79. Shibuta Y, Suzuki T (2010) Melting and solidification point of fcc-metal nanoparticles with respect to particle size: a molecular dynamics study. Chem Phys Lett 498(4–6): 323–327

80. Neyts EC, Shibuta Y, Van Duin ACT, Bogaerts A (2010) Catalyzed growth of carbon nanotube with definable chirality by hybrid molecular dynamics-force biased Monte Carlo simulations. ACS Nano 4(11): 6665–6672

81. Neyts EC, Van Duin ACT, Bogaerts A (2011) Changing chirality during single-walled carbon nanotube growth: a reactive molecular dynamics/Monte Carlo study. J Am Chem Soc 133(43): 17225–17231

82. Neyts EC, Van Duin ACT, Bogaerts A (2012) Insights in the plasma-assisted growth of carbon nanotubes through atomic scale simulations: effect of electric field. J Am Chem Soc 134(2): 1256–1260

83. Hatakeyama R, Kaneko T, Kato T, Li YF (2011) Plasma-synthesized single-walled carbon nanotubes and their applications. J Phys D Appl Phys 44(17):174004

84. Kato T, Hatakeyama R (2006) Formation of freestanding single-walled carbon nanotubes by plasma-enhanced CVD. Chem Vap Depos 12(6):345–352